

Empirical calibration of the sulphur valence oxygen barometer from natural and experimental glasses: method and applications

S. J. MATTHEWS*, D. H. S. MONCRIEFF AND M. R. CARROLL

Department of Earth Sciences, University of Bristol, Wills Memorial Building, Queens Road, Bristol, BS8 1RJ, UK

ABSTRACT

New data on sulphur valence and magmatic oxidation state for Central Andean volcanic rocks, in combination with published data for experimental and natural samples, allow derivation of a simple relationship between magma oxidation state and sulphur speciation. For a number of highly oxidized Central Andean volcanic rocks f_{O_2} has been calculated using magnetite-ilmenite or olivine-spinel pairs and the sulphur valence in glasses has been measured using the peak shift of S- $K\alpha$ radiation relative to a pyrite standard. Previously published experimental and natural data have been incorporated with a wider range in f_{O_2} and S valence. The variation in sulphur speciation (as S^{2-} or SO_4^{2-}) as a function of $\log f_{O_2}$ is described by an empirical polynomial fit which reproduces the data to within ± 0.5 log units and allows use of electron microprobe measurements of the S- $K\alpha$ wavelength shift for estimation of magmatic oxygen fugacities. This approach is applicable for f_{O_2} between FMQ-2 and FMQ+6, encompassing most terrestrial magmas. The method has been used to calculate the f_{O_2} conditions under which melt inclusions were trapped in andesitic magmas before magma mixing in two Central Andean volcanoes, and to calculate the oxygen fugacity of a slowly-cooled pyroclastic flow in which the Fe-Ti oxide phases have subsequently re-equilibrated. In combination with Fe-Ti oxide data, two distinct trends emerge for Lascar volcano. Basaltic andesite-andesitic magma chambers follow T - f_{O_2} trends which parallel the FMQ buffer curve, indicating ferrous-ferric iron buffering of oxygen fugacity. Dacitic anhydrite-bearing magmas with admixed basaltic andesite and andesite follow trends of increasing f_{O_2} with decreasing temperature, indicative of buffering of f_{O_2} by SO_2 - H_2S in a co-magmatic gas phase. This trend continues into the metamorphic aureole of the magma chamber, resulting in highly oxidized (close to magnetite-hematite) conditions.

KEY WORDS: sulphur valence, silicate melts, oxygen fugacity.

Introduction

THE valence of S in magmas depends to a large extent on magmatic oxidation state (e.g. Katsura and Nagashima, 1974; Carroll and Rutherford, 1987; 1988). At oxygen fugacities $< 2 \log f_{O_2}$ units below the fayalite-magnetite-quartz buffer (FMQ-2) S exists almost entirely in the form of sulphide, but with increasing f_{O_2} sulphate becomes increasingly abundant. In the range FMQ+1 to FMQ+2 a rapid increase in the proportion of sulphate occurs, reaching 90% of the total

dissolved sulphur by FMQ+2 (Carroll and Rutherford, 1988). This explains the occurrence of anhydrite phenocrysts in highly oxidized calc-alkaline magmas (Carroll and Rutherford 1987; Luhr 1990; Matthews *et al.*, 1994*a,b*). Published experimental data (Carroll and Rutherford, 1988) and data from natural back-arc magmas (Nilssen and Peach, 1993) and oceanic basalts (Wallace and Carmichael, 1994) are supplemented in this paper by analyses of S valence in glass inclusions from Andean rocks whose magmatic oxygen fugacities are estimated from mineral equilibria. Glasses have been analysed from two volcanic centres in the Andes of northern Chile. These are Lascar Volcano, an active andesitic-dacitic stratovolcano, and Cerro Overo, a young basaltic maar crater.

* Present address: Servicio Nacional de Geología y Minería, Avenida Santa María 0104, Casilla 10465, Santiago, Chile.

Geology of Lascar volcano, Cerro Overo and Cerro Tumisa

Lascar volcano (23°22'S, 67°44'W) is a Pleistocene-Recent calc-alkaline volcanic complex. Its eruptive history is described by Gardeweg *et al.* (1998). The evolution of Lascar involves four main stages of activity. Stage I (<43 ka) produced a stratocone and associated andesitic lava flows and pyroclastic flow deposits. Stage II was initiated by a shift in the eruptive centre to the west and the formation of an andesitic dome complex (Piedras Grandes dome complex) and associated block-and-ash flow deposits (Piedras Grandes deposit). A large explosive event partially or wholly demolished this edifice and produced the andesitic to dacitic Soncor ignimbrite and associated plinian airfall deposit (26.5 ka). Stage III (19.2–9.2 ka) is represented by a stratocone constructed on the site of Stage II activity and the eruption of andesitic to dacitic lava flows and pyroclastic flow deposits. The final eruption of this centre produced the andesitic Tumbres pyroclastic flow deposit (9.2 ka). Stage IV followed a shift of the eruptive centre back over the site of Stage I and the eruption of an andesitic lava flow (7.1 ka). Three deep collapse craters formed in the old Stage I edifice, the westernmost of which is the site of historic and current activity (Matthews *et al.*, 1997). The most recent activity consists of vigorous degassing, dome formation and intermittent explosive eruptions. The petrology and geochemistry of Lascar ejecta were described by Matthews *et al.* (1994a) and the Piedras Grandes and Soncor ejecta were studied in detail by Matthews *et al.* (1998). The eruptive products fall into two groups. Two-pyroxene andesite lavas and pyroclastic ejecta are interpreted as the products of convecting magma chambers which received frequent influxes of basalt or basaltic andesite; magma mixing was efficient and temperatures remained high. Products of this type are represented by the Stage I deposits, the Tumbres ejecta and the 1986 and 1990 ejecta. More evolved andesitic to dacitic deposits (Stage II and probably the 1993 ejecta) are the products of zoned magma bodies which formed following remobilization of a pre-existing solid or semisolid protopluton by a mafic magma influx following a long period of quiescence.

Cerro Overo is a postglacial basaltic maar crater located 20 km SE of Lascar. It is emplaced through Mio-Pliocene ignimbrites and erupted a small amount of fine-grained basalt containing

phenocrysts of olivine and clinopyroxene with inclusions and microphenocrysts of Cr-spinel. This magma is interpreted to have risen rapidly from the lower crust without residing in an upper crustal magma chamber. Olivine-bearing basaltic andesite samples from both Lascar and Cerro Overo are used for calibration of the S valence oxygen barometer in this paper. Cerro Tumisa is a Pleistocene (2–<0.4 Ma) composite volcano consisting of domes, lava flows, block-and-ash flow deposits and occasional pumiceous ignimbrites (Gardeweg, 1988, 1991). Dacitic pumice samples were analysed using the calibrated oxygen barometer described in this paper.

Measurement of S valence in glasses

Sulphur valence was measured with a wavelength dispersive electron microprobe (EMP) using the wavelength shift of the S-K α peak relative to a pyrite standard. The wavelength shift of S-K α X-rays from sulphide (S²⁻) to sulphate (SO₄²⁻) has previously been measured by X-ray fluorescence as 1.33 eV (Faesler and Goehring, 1952) and by EMP as 1.43 eV (Kucha *et al.*, 1989), 1.47 eV (Kucha and Stumpfl, 1992) and 1.41 eV (Matthews *et al.*, 1994b). In this study a JEOL JXA-8600 microprobe was used, equipped with a PET crystal and controlled by the Link Systems Spectra Program. The peak shift of the S-K α X-rays from galena, pyrite, sulphur, sodium sulphite, sodium bisulphite and baryte standards was measured relative to pyrite using a PET crystal (2d = 8.742 Å) and the Spectra peak-peak program. An accelerating voltage of 15 kV and a beam current of 30 nA were used (except for S, Na₂SO₃ and Na₂S₂O₅ for which current was reduced to 5 nA); analysis spot size was 5 to 10 μ m. Between each unknown analysis the pyrite standard was also measured in order to minimize errors associated with reproducibility of the spectrometer position. Figure 1 shows the wavelength shift of S-K α radiation, measured relative to pyrite, for several samples with S of known valence. Multiple analyses of each standard were performed, including the pyrite. The variation about zero of the pyrite data indicates the uncertainty in the measurements. The peak shift (P , in eV) vs. S valence (V) data were fit by linear regression and yield:

$$V = 5.75 (\pm 0.08) P - 1.11 (\pm 0.04) \quad (1)$$

This fit to measured data indicates that the peak shift from sulphide to sulphate is 1.39 ± 0.03 eV,

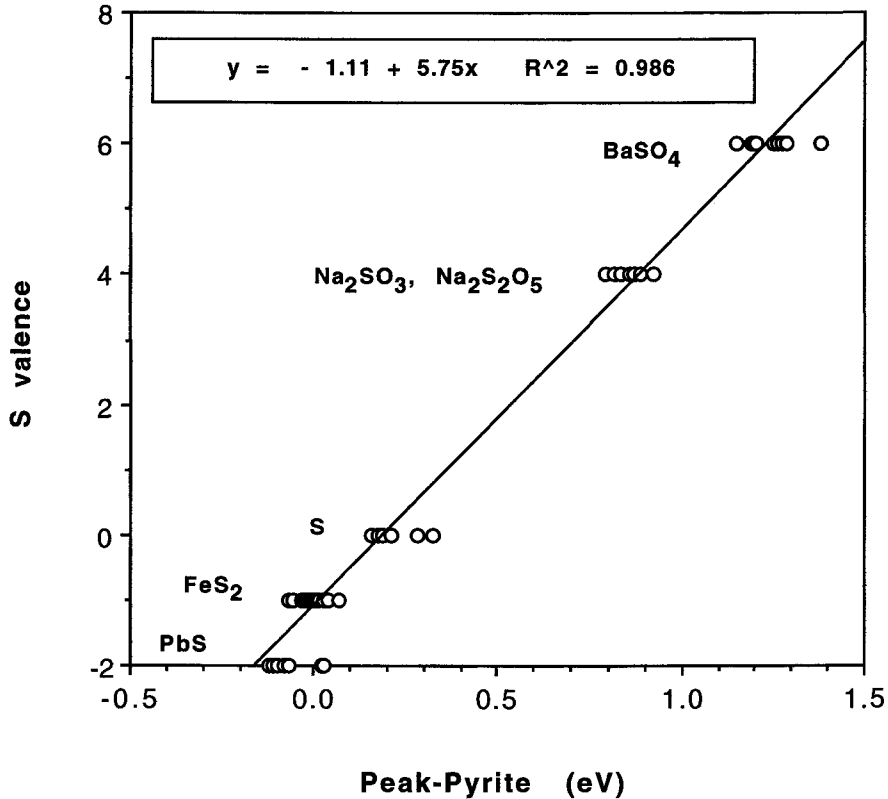


FIG. 1. Measured S-K α peak shifts relative to pyrite for various minerals and compounds.

in close agreement with previous measurements discussed above (1.33 to 1.47 eV).

The low S content of glass inclusions precludes use of the automated peak-peak routine for location of peaks and therefore a more sensitive, manual approach was adopted. A spectrometer scan was carried out across the entire peak from 2318.44 to 2300.97 eV using 50 intervals and counting for 25 to 30 s per interval. The same method was used for the pyrite standard but count times were reduced to 3 s per step. For both sample and standard measurements, a background interval either side of the peak was measured from 2406.29 to 2391 eV and 2275.29 to 2262.29 using 10 intervals for each side. A straight line was fitted to the background data and subtracted from the entire dataset in order to eliminate the background slope from the peak. A Gaussian curve was then fit to the peak with position, half-width, and height as free parameters. The uncertainty in peak position for S in degassed

matrix glasses (<100 ppm S) is usually unacceptably high, often exceeding the sulphide-sulphate peak shift. However, undegassed glass inclusions trapped within minerals typically have much higher S contents than the matrix glasses and therefore provide more useful samples for determining pre-eruptive sulphur speciation and concentration.

Oxygen fugacity determinations

Oxygen fugacities of magmas have been calculated using either magnetite-ilmenite pairs (Frost and Lindsley, 1992; Lindsley and Frost, 1992) or olivine-spinel pairs (Ballhaus *et al.*, 1990). For rapidly-cooled rocks (i.e. pumice and scoria) in which the two Fe-Ti oxides coexisted, 10–20 grains of both magnetite and ilmenite were analysed, and the magnetite and ilmenite were tested for equilibrium using Mg/Mn partitioning (Bacon and Hirschmann, 1988). Results are

TABLE 1. Calculated temperatures and oxygen fugacities of three evolved rocks from Lascar Volcano and Cerro Tumisa using Fe-Ti oxide pairs

Sample	Description	Temp °C	log(f_{O_2} /bar)	Δ FMQ
LASCAR, April 1993				
LAS182	2-Px. andesite	895	-10.41	2.44
Soncor Flow				
LAS191	Hbl. dacite	860	-10.60	2.91
LAS57	Hbl. dacite	898	-10.11	2.69
TUMISA				
SM9410	Hbl.-Bt. dacite	816	-11.25	3.15
SM9411	Hbl.-Bt. dacite	849	-11.60	2.13

presented in Tables 1 and 2. The olivine-spinel oxygen barometer was used for olivine basalt from Cerro Overo (SM9436) and a basaltic andesite from the Soncor ignimbrite of Lascar (LA124) at assumed temperatures of 1050 to 1150°C (range of temperatures obtained by 1-pyroxene thermometry; Frost and Lindsley, 1992; Lindsley and Frost, 1992) and pressures of 3–10 kbar. No significant pressure or temperature effects have been found in the calculation of Δ FMQ over this range. We estimate an error in calculated f_{O_2} of approximately 0.5 log units for this method. The Cerro Overo basaltic andesite data show an approximately 2 log unit decrease in f_{O_2} between Fo₈₇ and Fo₈₀, although there is some scatter in the data. The Lascar olivine basalt data suggest a slight increase in f_{O_2} with decreasing Fo (<1 log f_{O_2} unit between Fo₈₇ and Fo₈₀). Straight lines were fitted to the data and the resulting relationships between olivine Fo content and oxygen fugacity were used to calculate the f_{O_2} for glass inclusions by analysing the olivine host adjacent to the inclusion. This was necessary since not all olivines containing glass inclusions also contained spinels, and often spinels occurred in different growth zones of the host olivine to the glass inclusions, so that direct calculation of f_{O_2} in glass inclusions was not possible.

Results

For glass inclusions in olivines from Cerro Overo (Sample SM9436) there is a positive correlation between olivine Fo (and therefore f_{O_2}) and S valence (Fig. 2). These olivines, having calculated oxygen fugacities ranging from FMQ+1.0 to +1.4, (estimated error of ± 0.5 log units) contain glass inclusions with a wide range in S valence

(0.08–0.79; Table 3), consistent with the experimental data of Carroll and Rutherford (1988) which indicate a sharp change in sulphur speciation in the f_{O_2} range FMQ+1 to FMQ+2. For the Lascar olivine basaltic andesite (Sample LA124) the olivines with Fo₈₀ have calculated oxygen fugacities around FMQ+2.0 to +2.1 and contain mainly oxidized sulphur (sulphate/total S = 0.81–0.88). However, glass inclusions in some more Fe-rich olivines from Lascar have lower abundance of sulphate, despite having higher calculated f_{O_2} (open squares in Fig. 2). Closer inspection of these glass inclusions revealed that

TABLE 2. Calculated oxygen fugacities for olivine-spinel pairs from two Andean olivine basalts

Sample	Fo (olivine)	f_{O_2} (1100°C)	Δ FMQ
Lascar LA124			
O1 core	86.4	-8.20	1.47
O1 core	86.4	-8.58	1.08
O1 core	86.4	-8.60	1.06
O4 core	86.1	-7.87	1.79
O9 core	83.0	-7.70	1.97
O9 rim	81.9	-7.82	1.84
O9 rim	81.9	-7.92	1.75
Co. Overo SM9436			
O2	86.0	-7.37	2.29
O3	85.1	-8.88	0.78
O3	85.1	-7.96	1.70
O4 core	84.1	-9.31	0.35
O4 rim	82.9	-8.72	0.94
O4 rim	82.9	-8.80	0.86
O5	82.6	-8.86	0.80
O5	82.6	-8.94	0.72

CALIBRATION OF THE S VALENCE O BAROMETER

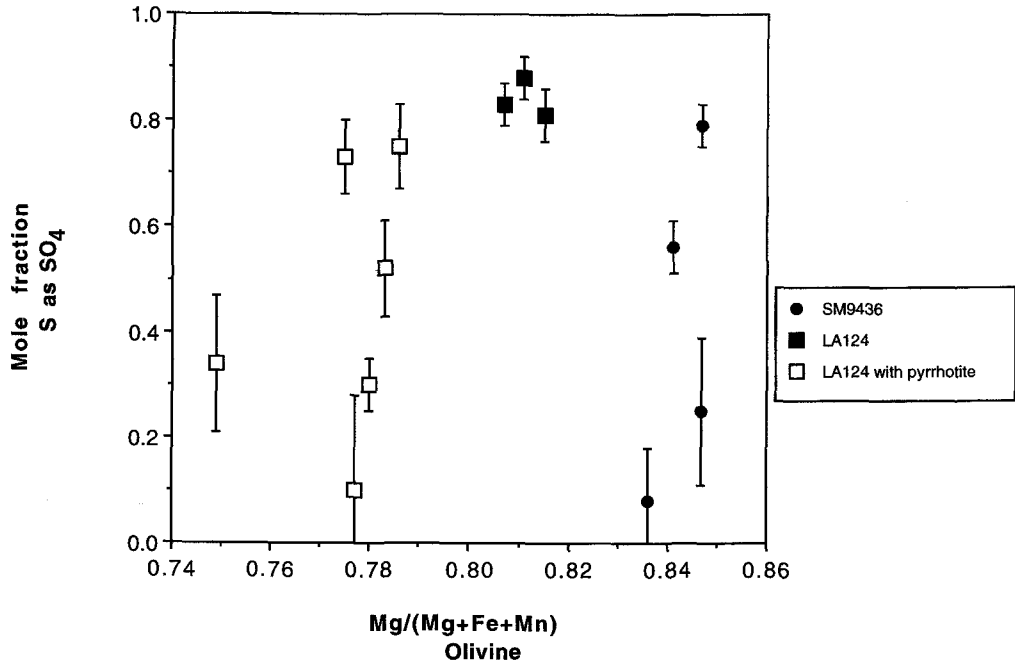


FIG. 2. Relation between olivine composition and S valence in glass inclusions in olivine phenocrysts. Filled circles; Cerro Overo basaltic andesite. Squares, Soncor basaltic andesite — filled: fresh glass inclusions; open: glass inclusions with secondary pyrrhotite.

TABLE 3. Measured S valence of glass inclusions and calculated oxygen fugacity of either host olivines from olivine-spinel pairs or whole rock from Fe-Ti oxides

Sample	Description	Host mineral	Fo (olivine)	Molar $SO_4/\Sigma S$	ΔFMQ	Method
CO. OVERO						
SM9436	Olivine basaltic andesite					
G1		Olivine	83.6	0.08 ± 0.10	0.99	Olivine compn.
G2		Olivine	84.7	0.25 ± 0.14	1.38	Olivine compn.
G3		Olivine	84.7	0.79 ± 0.04	1.38	Olivine compn.
G4		Olivine	84.1	0.56 ± 0.05	1.17	Olivine compn.
LASCAR: Soncor ignimbrite						
LA124	Olivine basaltic andesite					
Glass5		Olivine	80.7	0.83 ± 0.04	2.10	Olivine compn.
Glass7		Olivine	81.5	0.81 ± 0.05	1.99	Olivine compn.
Glass8		Olivine	81.1	0.88 ± 0.04	2.04	Olivine compn.
LAS191	Hornblende andesite					
Glass12		Hornblende	—	0.77 ± 0.11	2.91	Magnetite-ilmenite
LASCAR: April 1993 Eruption						
LAS182	2-pyroxene andesite					
Glass10		Pyroxene	—	0.82 ± 0.10	2.44	Magnetite-ilmenite
Glass11		Pyroxene	—	0.84 ± 0.10	2.44	Magnetite-ilmenite

they contained tiny crystals of magnetite and iron sulphide, presumably formed following entrapment of the inclusion; we do not consider such samples affected by post-entrapment crystallization to be reliable for determination of primary S valence. Only glass inclusions in olivine more magnesian than Fo₈₀ were used in the S valence-*f*O₂ calibration.

For more evolved, oxidized (FMQ+2.4 to +2.9), anhydrite-bearing Lascar magmas with Fe-Ti oxide data the measured sulphate/total S is 0.71–0.84, in agreement with the data of Carroll and Rutherford (1988). The entire dataset for natural and experimental glasses can be described (Fig. 3) by a polynomial equation of the form:

$$\Delta\text{FMQ} = a.S^5 + b.S^4 + c.S^3 + d.S^2 + e.S + f \quad (2)$$

Where:

$$S = \text{Mole fraction S as sulphate} = (V + 2)/8$$

(*V* from Eqn 1)

$$a = 227.55, b = -532.83, c = 464.77, \\ d = -186.88, \\ e = 36.563 \text{ and } f = -1.8793 \quad (R^2 = 0.857)$$

Use of lower order polynomials resulted in poor fits to the data, especially at the high and low *f*O₂ ends of the data. Equation 2 appears to be applicable to a wide range of magma compositions (dry basalts to hydrous dacites) at oxygen fugacities between FMQ–2 and FMQ+6. The region with a low slope (FMQ+1 to FMQ+2) will provide the highest accuracy since in this part of the graph the calculated *f*O₂ is less sensitive to the measured S valence. It can only be applied, however, to magmas whose glass inclusions contain sufficient sulphur to reduce the error in the measurement of sulphur valence (typically >200–300 ppm S).

Although our treatment of the relation between oxidation state and sulphur speciation is not based on thermodynamic considerations, this empirical approach describes data over a wide range of *f*O₂ better than available thermodynamic-based treatment. For example, Wallace and Carmichael (1994) tried to model S redox equilibria in melts using the reaction:

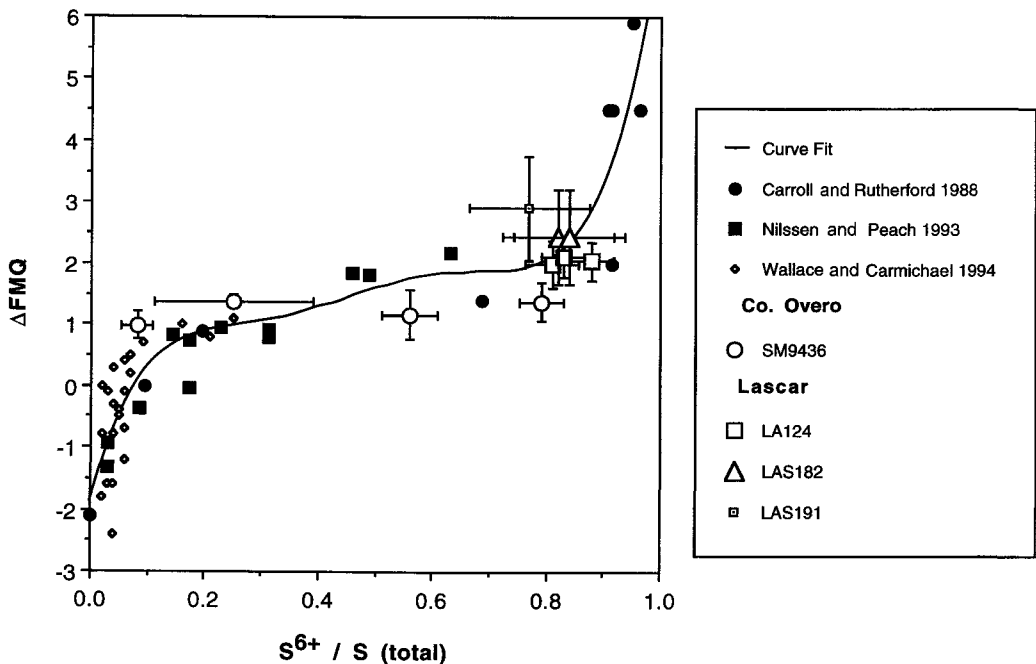
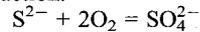


FIG. 3. Relation between calculated oxygen fugacity (ΔFMQ) and measured S valence in glasses from Lascar and Cerro Overo samples and published natural samples and experimental data. The curve shows polynomial fit to the data, described in the text. Error bars are omitted from published data for clarity.

for which the equilibrium constant, assuming activities equal to mole fractions, is:

$$K = XSO_4^{2-} / (XS^{2-})(f_{O_2}^2)$$

With rearrangement and description of f_{O_2} relative to the FMQ buffer, this yields:

$$\Delta FMQ = 0.5 \log (XSO_4^{2-} / XS^{2-}) - 0.5 \log K - FMQ$$

or,

$$\Delta FMQ = 0.5 \log (XSO_4^{2-} / XS^{2-}) + a/T - FMQ (T)$$

Therefore, a plot of ΔFMQ against $\log (XSO_4^{2-} / XS^{2-})$ should yield a straight line with a slope of 0.5. In fact, as Wallace and Carmichael (1994) found, the data do not fall on a straight line but retain their S-shape in such a plot, which has a best-fit straight line with a slope of 1.68 (Fig. 4). The inability of this model to adequately describe the behaviour of S in melts at high and low oxygen fugacities may reflect the presence of other sulphur species (e.g. S^{-} , S^0 and S^{4+}), complexing effects within the melt (e.g. Haughton *et al.*, 1974), and the inadequacy of the assumption that activity coefficients, or their ratio, remain constant.

Applications

The relationship between S valence and melt oxidation state provides a means of estimating oxygen fugacity from electron microprobe measurement of the wavelength shift of S- $K\alpha$ X-rays, and is therefore applicable to situations where the estimation of oxidation state by more conventional means is not possible. We illustrate the utility of this approach with two examples. The first is the identification of differences in oxidation state recorded by glass inclusions in minerals from mixed magmas. This is particularly applicable to Central Andean stratovolcanoes such as Lascar whose oxidized, dacitic magma chambers have experienced repeated influxes of more reduced mafic magma (Matthews *et al.*, 1994a,b, 1998). Previously it was difficult to determine the f_{O_2} of the injected magma or the pre-existing host magma due to the re-equilibration of Fe-Ti oxides during subsequent fractional crystallization. The second problem is the determination of magma oxidation state from slowly-cooled lavas whose Fe-Ti oxides have re-equilibrated following eruption. In this case, measurement of sulphur wavelength shifts for melt inclusions may provide information on pre-eruptive magmatic oxidation state (assuming the

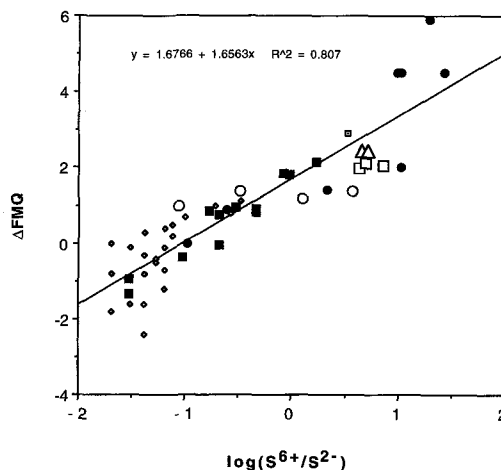


FIG. 4. Plot of ΔFMQ against $\log (XSO_4^{2-} / XS^{2-})$ for the same data as in Fig. 3. The S-shaped relationship indicates that a simple thermodynamic treatment does not adequately describe the data.

inclusions have not experienced post-entrapment crystallization).

Example 1

Examples of two mixed calc-alkaline magmas have been studied in order to compare the oxygen fugacities of glass inclusions in pre-mixing phases with that estimated from magnetite-ilmenite compositions. The first rock is an andesitic hornblende-rich scoria from a mixed andesitic-dacitic eruption of Lascar Volcano; the Soncor flow (Matthews *et al.*, 1994a; Gardeweg *et al.*, 1994, 1998). The second is represented by two hornblende-biotite pumice clasts from a mixed andesitic-dacitic eruption of the nearby 2 m.y. old Cerro Tumisa (Gardeweg 1988). Oxygen fugacities of glass inclusions in amphiboles from these two magmas have been calculated from their measured S valence (Table 4) using equation 2. These calculated oxygen fugacities range from FMQ+1 to FMQ+1.8, and are at odds with the results of the magnetite-ilmenite calculations for the magmas (FMQ+2.13 to +3.15). The hornblendes in these samples are interpreted to have originated in more reduced mafic magmas which suffered quenching and oxidation on injection into their respective dacitic magma chambers (Matthews *et al.*, 1994a,b). In fact, the calculated oxygen fugacities of these mafic magmas are

TABLE 4. Calculated oxygen fugacities of glass inclusions in phenocryst phases from two mixed magmas, compared with that calculated for the rocks using magnetite-ilmenite pairs

Sample	Host phase	Molar $\text{SO}_4/\Sigma\text{S}$	ΔFMQ (calc.)	ΔFMQ (Mtt-Ilm)
LAS57 ^a				
Glass11	Hornblende	0.34 ± 0.09	1.11 (+0.23 -0.16)	2.69
Glass12	Interstitial*	0.69 ± 0.08	1.82 (+0.09 -0.06)	2.69
Glass11	Hornblende	0.32 ± 0.19	1.07 (+0.52 -0.55)	2.69
SM9410 ^b				
Glass1	Hornblende	0.45 ± 0.15	1.39(+0.35 -0.36)	3.15
SM9411 ^b				
Glass2	Hornblende	0.55 ± 0.14	1.66 (+0.16 -0.38)	2.13

^a - samples from Lascar^b - samples from Tumisa

* - interstitial glass in a hornblende crystal clot

remarkably consistent and agree with the data from the nearby Cerro Overo olivine basalt, suggesting a similarity in source magma oxidation state between the three volcanic centres.

It is concluded that the mafic magmas, unable to degas their dissolved sulphur, were buffered by the ferrous-ferric iron equilibrium at FMQ+1 to 1.5 (flatter region of the curve in Fig. 3) until they entered the subvolcanic magma chamber. This contrasts with the model of Matthews *et al.* (1994b) for the later mixed magmas from which most of the sulphur has been exsolved and whose higher oxygen fugacities are thought to have been buffered by the $\text{H}_2\text{S}-\text{SO}_2$ equilibrium in the coexisting gas phase. The reason for this difference may be that the mafic magmas resided at higher pressures prior to injection into the higher level magma chambers and much of their sulphur remained in solution until this event.

Example 2

The 9000 yr b.p. andesitic Tumbres flow of Lascar (Matthews *et al.*, 1994a, Gardeweg *et al.*, 1994) contains Fe-Ti oxide phases which are unsuitable for the calculation of f_{O_2} due to their wide compositional range and post-eruptive re-equilibration. In addition, it is rich in skarn xenoliths, some of which have suffered partial melting (Matthews *et al.*, 1996). Glass inclusions in minerals from two scoria samples have been analysed to determine their sulphur valence and in turn the f_{O_2} under which they were trapped. These samples are a scoria clast from a pyroclastic flow lobe (LAS13) and a clast from the plinian

airfall deposit which underlies the flow (LAS1). In addition, interstitial glasses from a partially melted skarn xenolith from this flow unit (LA111), and a biotite pumice clast (LA117) were analysed for comparison with the host magma. In the case of LAS1 and LA117, glass inclusions in orthopyroxene phenocrysts also allowed the determination of temperature (from one-pyroxene thermometry), and thus, absolute f_{O_2} . Results are listed in Table 5 and presented in Fig. 5.

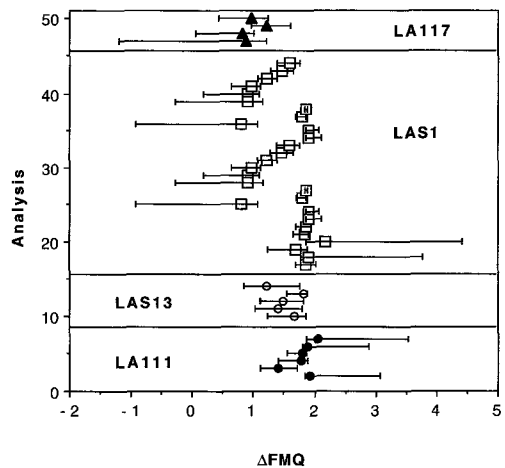


FIG. 5. Calculated oxygen fugacities of glass inclusions from S valence measurements in various samples from the Tumbres flow deposit, Lascar volcano. LA111: buchite xenolith; LAS13, LAS1: basaltic andesite scoria; LA117: biotite dacite pumice.

CALIBRATION OF THE S VALENCE O BAROMETER

TABLE 5. Calculated oxygen fugacities of glass inclusions in phenocryst phases from two scoria clasts and interstitial glasses from a partially melted skarn xenolith (buchite) from the andesitic Tumbres flow

Sample	Host phase	Molar $SO_4/\Sigma S$	ΔFMQ (calc.)	Temp °C	Log f_{O_2}
LA111	Xenolith				
Glass1	Interstitial glass	0.76 ± 0.13	+1.92 (+1.18 -0.13)	n.d.	n.d.
Glass2	Interstitial glass	0.44 ± 0.11	+1.37 (+0.29 -0.28)	n.d.	n.d.
Glass3	Interstitial glass	0.59 ± 0.15	+1.73 (+0.13 -0.37)	n.d.	n.d.
Glass4	Interstitial glass	0.60 ± 0.11	+1.75 (+0.09 -0.24)	n.d.	n.d.
Glass5	Interstitial glass	0.74 ± 0.15	+1.86 (+1.05 -0.13)	n.d.	n.d.
Glass6	Interstitial glass	0.80 ± 0.11	+2.07 (+1.47 -0.24)	n.d.	n.d.
LAS13	Scoria				
Glass1	Pyroxene	0.53 ± 0.15	+1.61 (+0.20 -0.42)	n.d.	n.d.
Glass2	Pyroxene	0.44 ± 0.16	+1.37 (+0.38 -0.37)	n.d.	n.d.
Glass3	Pyroxene	0.47 ± 0.14	+1.45 (+0.31 -0.37)	n.d.	n.d.
Glass4	Pyroxene	0.61 ± 0.12	+1.76 (+0.09 -0.25)	n.d.	n.d.
Glass5	Plagioclase	0.37 ± 0.20	+1.17 (+0.53 -0.40)	n.d.	n.d.
LAS1	Scoria				
Glass5	Plagioclase	0.67 ± 0.13	+1.81 (+0.21 -0.17)	n.d.	n.d.
Glass6	Plagioclase	0.75 ± 0.17	+1.89 (+1.91 -0.16)	n.d.	n.d.
Glass7	Plagioclase	0.54 ± 0.16	+1.64 (+0.19 -0.44)	n.d.	n.d.
Glass9	Plagioclase	0.82 ± 0.12	+2.20 (+2.22 -0.36)	n.d.	n.d.
Glass11	Plagioclase	0.64 ± 0.12	+1.79 (+0.10 -0.20)	n.d.	n.d.
Glass12	Plagioclase	0.66 ± 0.12	+1.81 (+0.14 -0.17)	n.d.	n.d.
G30	Orthopyroxene	0.75 ± 0.06	+1.91 (+0.21 -0.04)	818	-12.45
G31	Orthopyroxene	0.75 ± 0.06	+1.90 (+0.17 -0.03)	818	-12.46
G32	Orthopyroxene	0.17 ± 0.14	+0.80 (+0.27 -1.72)	804	-13.86
G33	Orthopyroxene	0.60 ± 0.06	+1.81 (+0.05 -0.11)	818	-12.55
G34	Orthopyroxene	0.68 ± 0.05	+1.87 (+0.02 -0.02)	818	-12.50
G35	Orthopyroxene	0.21 ± 0.15	+0.91 (+0.25 -1.18)	804	-13.75
G36	Orthopyroxene	0.21 ± 0.12	+0.91 (+0.19 -0.72)	951	-10.97
G37	Orthopyroxene	0.24 ± 0.10	+0.96 (+0.15 -0.32)	794	-13.91
G38	Orthopyroxene	0.37 ± 0.06	+1.21 (+0.17 -0.13)	950	-10.69
G39	Orthopyroxene	0.46 ± 0.06	+1.47 (+0.18 -0.18)	950	-10.43
G40	Orthopyroxene	0.50 ± 0.07	+1.59 (+0.17 -0.21)	985	-9.74
LA117	Biotite dacite				
Glass1	Orthopyroxene	0.20 ± 0.18	+0.89 (+0.32 -2.08)	736	-15.33
Glass2	Orthopyroxene	0.18 ± 0.10	+0.83 (+0.19 -0.77)	749	-15.07
Glass3	Orthopyroxene	0.37 ± 0.14	+1.21 (+0.41 -0.24)	699	-15.95
Glass4	Orthopyroxene	0.25 ± 0.14	+0.98 (+0.25 -0.56)	721	-15.62

Two main conclusions can be drawn from these data. Firstly, oxygen fugacity (relative to FMQ) remains roughly constant for all pyroxene temperatures in both the host magma and the biotite pumice ($\Delta FMQ = +0.8$ to $+2.2$). Subsolidus temperatures calculated for the pyroxenes in the biotite pumice indicate that this also represents a partially melted xenolith. This behaviour is attributed to ferrous-ferric iron buffering of f_{O_2} .

Secondly, the calculated oxygen fugacities of interstitial partial melts in the xenolith LA111 lie within the range of the two magmatic samples, indicating that f_{O_2} during melting was buffered by the host magma. The actual oxygen fugacities under which the skarn formed are considered to have been much higher than that of the magma chamber, approaching the magnetite-hematite buffer (Matthews *et al.*, 1996).

The large positive error bars for calculated f_{O_2} above FMQ + 1.85 are the result of the uncertainties in measured S valence intersecting the steep part of the graph in Fig. 3. In this region the calculated f_{O_2} is highly sensitive to small changes in the measured S valence.

Conclusions

A fifth order polynomial fit to the relationship between S valence in glasses and calculated oxygen fugacity (relative to the FMQ buffer) provides a sensitive technique for the estimation of f_{O_2} in both experimental and natural S-bearing glasses and for tracking changes in f_{O_2} during complex magmatic processes. The estimated error in this approach is ± 0.5 log units, although the actual size of errors obtained depends upon the precision of S peak shift measurements, mainly influenced by the amount of S in the sample. Errors may be significantly larger at the high and low f_{O_2} ends of the f_{O_2} range investigated (FMQ-2 to FMQ+6). A thermodynamic treatment based on the presence of sulphide and sulphate as the only S-bearing species does not adequately describe the data, probably due to

inadequacies in our knowledge of activity-composition relations for S dissolved in melts. Measured S wavelength shifts for melt inclusions in Andean volcanic rocks, combined with more conventional geothermometry and measurements of coexisting Fe-Ti oxide compositions provide information on the evolution of oxidation state and the potential importance of magma mixing in influencing magma oxidation state. When S valence data are combined with magnetite-ilmenite thermometry for the whole of Lascar (Fig. 6), two trends emerge: (1) basaltic andesite-andesitic magmas (the Tumbres pyroclastic flow deposit and the 1986 and 1990 lavas) follow temperature- f_{O_2} trends which parallel the FMQ buffer curve, indicating ferrous-ferric iron buffering of oxygen fugacity. These magmas contain sulphide phenocrysts such as pyrrhotite and chalcopyrite; and (2) dacitic magma chambers with a smaller admixture of basaltic andesite and andesite exhibit a strong increase in f_{O_2} relative to FMQ with decreasing temperature and contain anhydrite phenocrysts. Examples are the Piedras Grandes and Soncor magmas, the Capricorn lava and the 19-20 April and 17 December 1993 products. These products are

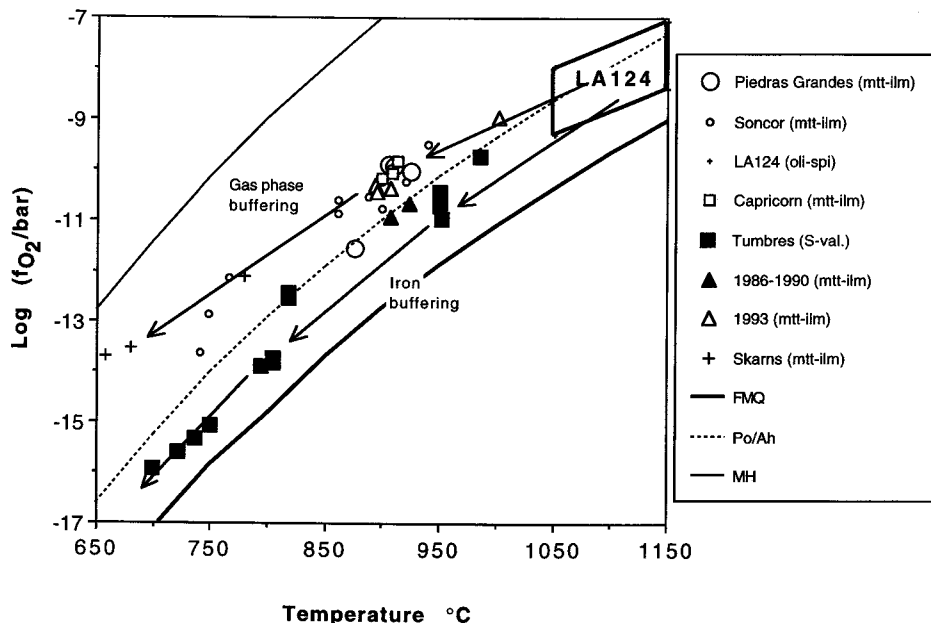


FIG. 6. Calculated temperatures and oxygen fugacities for Lascar magmas using magnetite-ilmenite (mtt-ilm), 1-pyroxene-olivine-spinel (oli-spi) and 1-pyroxene-S valence (S-val.) geothermobarometers. FMQ: fayalite-magnetite-quartz buffer; MH: magnetite-hematite buffer; Po/Ah: pyrrhotite-anhydrite (sulphide-sulphate) buffer.

thought to indicate buffering of f_{O_2} by a co-magmatic S-rich gas phase, as described by Matthews *et al.* (1994b). The rapid exsolution of S from the mafic magma on injection and quenching is thought to be responsible for this behaviour. Sulphur buffering of oxygen fugacity continues into the skarn zone and in low-temperature, slowly-cooled shallow intrusions from the magma chamber.

Acknowledgements

We are grateful to Moyra Gardeweg and the Fuerza Aerea de Chile for logistical support in Chile, and to Sergio Manquez and Sergio Palma for assistance in the field. This project was supported by NERC grant no. GR3/9047 and GR9/884. The paper was improved by helpful reviews from M. Henderson and an anonymous reviewer.

References

- Bacon, C.D. and Hirschmann, M.M. (1988) Mg/Mn partitioning as a test for equilibrium between coexisting Fe-Ti oxides. *Amer. Mineral.*, **73**, 57–61.
- Ballhaus, C., Berry, R.F. and Green, D.H. (1990) Oxygen fugacity controls in the earth's upper mantle. *Nature*, **348**, 437–40.
- Carroll, M.R. and Rutherford, M.J. (1987) The stability of igneous anhydrite: experimental results and implications for sulfur behaviour in the 1982 El Chichon trachyandesite and other evolved magmas. *J. Petrol.*, **28**, 781–801.
- Carroll, M.R. and Rutherford, M.J. (1988) Sulfur speciation in hydrous experimental glasses of varying oxidation state: Results from measured wavelength shifts of sulfur X-rays. *Amer. Mineral.*, **73**, 845–9.
- Faesler, A. and Goehring, M. (1952) Röntgenspektrum und Bindungszustand die α Fluoreszenzstrahlung des Schwefels. *Naturwissenschaften*, **39**, 169–77.
- Frost, B.R. and Lindsley, D.H. (1992) Equilibria among Fe-Ti oxides, pyroxenes, olivine, and quartz: Part II. Application. *Amer. Mineral.*, **77**, 1004–20.
- Gardeweg, M. (1988) Petrografia y geoquímica del complejo volcánico Tumisa, Altiplano de Antofagasta, Andes del Norte de Chile. Congreso Geológico Chileno, 5. *Servicio Nacional de Geología y Minería, Chile*, pp. 183–208.
- Gardeweg, M.C. (1991) *The geology, petrology and geochemistry of the Tumisa Volcanic Complex, North Chile*. Unpub. PhD. Thesis, Kingston Polytechnic. 374 pp.
- Gardeweg, M.C., Fuentealba, G., Murillo, M. and Petit-Breuhl, M.E. (1994) Volcan Lascar: Geología y Evaluación del Riesgo Volcánico-Altiplano II Región. *Informe Registrado, 1994-3, Biblioteca Servicio Nacional de Geología y Minería, Chile*. 169 pp.
- Gardeweg, M.C., Sparks, R.S.J. and Matthews, S.J. (1998) Evolution of Lascar Volcano, Northern Chile. *J. Geol. Soc., Lond.*, **155**, 89–104.
- Haughton, D.R., Roeder, P.L. and Skinner, B.J. (1974) Solubility of sulfur in mafic magmas. *Econ. Geol.*, **69**, 451–67.
- Katsura, T., Nagashima, S. (1974) Solubility of sulfur in some magmas at 1 atmosphere. *Geochim. Cosmochim. Acta*, **38**, 517–31.
- Kucha, H. and Stumpfl, E.F. (1992) Thiosulphates as precursors of banded sphalerite and pyrite at Bleiberg, Austria. *Mineral. Mag.*, **56**, 165–72.
- Kucha, H., Wouters, R. and Arkens, O. (1989) Determination of sulfur and iron valence by microprobe. *Scanning Microsc.*, **3**, 89–97.
- Lindsley, D.H. and Frost, B.R. (1992) Equilibria among Fe-Ti oxides, pyroxenes, olivine, and quartz: Part I. Theory. *Amer. Mineral.*, **77**, 987–1003.
- Luhr, J.F. (1990) Experimental phase relations of water- and sulfur-saturated arc magmas and the 1982 eruptions of El Chichon volcano. *J. Petrol.*, **31**, 1071–114.
- Matthews, S.J., Jones, A.P. and Gardeweg, M.C. (1994a) Lascar Volcano, Northern Chile; Evidence for Steady-State Disequilibrium. *J. Petrol.*, **35**, 401–32.
- Matthews, S.J., Jones, A.P. and Beard, A.D. (1994b) Buffering of melt oxygen fugacity by sulphur redox reactions in calc-alkaline magmas. *J. Geol. Soc., Lond.*, **151**, 815–23.
- Matthews, S.J., Marquillas, R.A., Kemp, A.J., Grange, F.K. and Gardeweg, M.C. (1996) Active Skarn Formation Beneath Lascar Volcano, Northern Chile: A Petrographic and Geochemical Study of Xenoliths in Eruption Products. *J. Metam. Geol.*, **14**, 509–30.
- Matthews, S.J., Gardeweg, M.C. and Sparks, R.S.J. (1997) The 1984 to 1996 cyclic activity of Lascar volcano, northern Chile: cycles of dome growth, dome subsidence, degassing and explosive eruptions. *Bull. Volcanol.*, **59**, 72–82.
- Nilsson, K. and Peach, C. (1993) Sulfur speciation, oxidation state, and sulfur concentration in backarc magmas. *Geochim. Cosmochim. Acta*, **57**, 3807–13.
- Wallace, P.J. and Carmichael, I.S.E. (1994) S speciation in submarine basaltic glasses as determined by measurements of SKa X-ray wavelength shifts. *Amer. Mineral.*, **79**, 161–7.

[Manuscript received 19 March 1998;
revised 9 September 1998]